

**SUMMARY**

Using sonic well logs from diverse geological environments, we analyze the statistics of the lithological layers relevant to seismic wave propagation and use localization theory to calculate the frequency-dependent apparent attenuation caused by random scatterings. As measured by  $Q^{-1}$ , this attenuation has a peak at 50-150 Hz, corresponding to a localization length of 1-3 miles and a  $Q$  value of 120-450. At 20 Hz the attenuation is smaller, with localization length in the range of 10-20 miles and an apparent  $Q$  of 300-700. These values of  $Q$  are consistent with previous calculations based on well-log data (Schoenberger and Levin, 1978; Menke, 1983). We observe dispersion effect in the form of a progressive phase-delay between the wave-equation and the primaries-only synthetic traces and offer a qualitative explanation of this phenomenon. The power spectral density of the trace is also computed for different time gates and compared with localization theory predictions. The non-white, quadratic frequency dependence of the spectrum is observed as predicted by theory. Furthermore, when plotted as a function of the scaled variable that is inversely proportional to the localization length, the average of the different spectra exhibits excellent agreement with the dimensionless scaling function as derived theoretically.

**INTRODUCTION**

Multiple scattering of seismic waves is a topic of numerous past studies (O'Doherty and Anstey, 1971; Schoenberger and Levin, 1974, 1978; Richards and Menke, 1983; Menke, 1983). The results of these studies clearly indicate that the cumulative effect of multiple scattering is equivalent to an apparent attenuation of the wave. An alternative formulation of this random-scattering attenuation phenomena can be found in the localization theory, originally proposed by P. W. Anderson (Anderson, 1958) in the context of electron diffusion in disordered materials. In recent years, implications of the localization theory for elastic and electromagnetic wave propagation and scattering in randomly stratified media have been investigated both analytically and numerically (Sheng, White, Zhang, and Papanicolaou, 1986; Burridge, Papanicolaou, and White, 1987; Sheng, Zhang, White, and Papanicolaou, 1986; White, Sheng, Zhang, and Papanicolaou, 1987). It is found that for the single-frequency wave the multiple-scattering attenuation length  $\ell$ , or the localization length, has the general property that  $\ell \sim \nu^{-2}$  at low frequencies and that over the whole frequency range it is always bounded below by a well-defined minimum value for any given random medium. In addition, for pulse propagation the localization theory predicts a generic time-domain characteristic linking the power spectrum of the back-scattered coda and the localization length  $\ell$ . It is the purpose of the present paper to examine the statistics of the well-logs and to study their wave propagation and scattering characteristics in the

framework of the localization theory. We show that the  $Q^{-1}$  due to multiple scattering has a peaked form, with the values of  $\ell$  obtained at seismic frequencies consistent with previous observations. To assess the effect of multiple scattering, we also calculated the wave equation solution and the primaries-only synthetics for a 20-Hz pulse. Comparison of the two shows that the main difference is in the form of a small progressive phase difference accountable by a velocity correction. The statistics of the back-scattered coda is also calculated and found to be in good agreement with theoretical predictions.

**SONIC-LOG STATISTICS**

Sonic logs of four wells--Federal, Hornbeck, Strawberry, and Inigok--were analyzed with respect to their mean, variance, and autocorrelation. The logs are unblocked, with minimum data interval of 1 ft. Since the density is relatively constant as seen from the density logs, it is set at a constant value of  $2\text{g/cm}^3$  in all our calculation. By writing the compressibility  $K^{-1}$  as  $K^{-1}(z) = K_0^{-1}(z) [1 + \sigma(z)]$ , the mean compressibility  $K_0^{-1}$  is calculated by using a moving Parzen window of 1500 ft. The relative variance  $\langle \sigma^2(z) \rangle$  is also calculated, where the angular brackets denotes Parzen-window averaging. Both  $K_0^{-1}$  and the relative variance may be characterized by a decreasing trend with increasing depth, implying a more consolidated and smoother medium deeper down. The autocorrelation function, defined as  $\langle \sigma(z)\sigma(z+\Delta) \rangle / \langle \sigma^2(z) \rangle$ , yields surprisingly good exponential form with a correlation length on the order of 5-10 ft. A typical result is shown in Figure 1 together with the best exponential fit. We note that the exponential correlation of the sonic well logs has been observed before (Godfrey, Muir, and Rocca, 1980); however, the prevalence of this behavior is surprising.

**ATTENUATION OF SINGLE-FREQUENCY WAVES**

For a randomly-stratified half-space, one can define the multiple-scattering attenuation length, or the localization length  $\ell$ , as

$$\ell = -\overline{[\ln T]}/L, \quad (1)$$

where  $T$  is the transmitted wave amplitude at distance  $L$  from the half-space interface, and the bar denotes averaging over random configurations. It should be noted that in contrast to the attenuation length arising from deterministic dissipation mechanisms, the apparent attenuation is statistical in character. That is, the exponential decay of the wave envelope over distances large compared with  $\ell$  is generally accompanied by amplitude fluctuations on smaller distance scales.

The localization length defined in the above manner is a frequency-dependent quantity. Recently, analytical study using stochastic differential equations and numerical simulations have determined

(Sheng, White, Zhang, and Papanicolaou, 1986) that to the leading order,  $\ell^{-1}$  behaves as  $\nu^2$  in the low frequencies and saturates to a constant as frequency  $\nu$  increases. Overall, the form

$$\ell(\nu) = C_1 + \frac{C_2}{\nu^2} \quad (2)$$

gives an accurate description of the localization length frequency dependence. To test this prediction, we use transfer-matrix method in the frequency domain to calculate  $T$  for each of the four wells in the range of  $\nu=1-7000$  Hz. The  $\ell^{-1}$  is then evaluated as  $|\ln T|/L$ . Figure 2 shows the typical result for one of the wells and the best fit to the data using the form of Eq.(2). It is seen that while there is significant fluctuations in the data, yet the overall trend is well-described by the theory. Physically, the  $\nu^2$  dependence of  $\ell^{-1}$  has its origin in the  $\nu^2$  frequency variation of Rayleigh scattering for stratified media. Analytical theory has shown that the constant  $C_2$  is related to the integral of the correlation function for  $\sigma$ , i.e.

$$C_2 = \langle \sigma^2 \rangle / 2\pi^2 \alpha^{-1}, \quad (3)$$

where  $\alpha$  is the averaged integral of  $\langle \sigma(z)\sigma(z+\Delta) \rangle$ . It should be noted that by adapting Eq.(3) to the case of random layerings of equal thickness, we recover exactly the formula by Menke (Menke, 1983). However, we differ from Menke in that our  $\ell(\nu)$  saturates to a fixed value at high frequencies. This frequency independence, plus a lower bound for the constant  $C_1$ , may be seen as follows. For  $\nu \rightarrow \infty$ , the phase incoherence of the individual scattering events means that  $|T|^2$  may be approximated by the product of  $(1-r_i^2)$ , where  $r_i$  is the reflection coefficient at interface  $i$ . Since  $r_i$  is frequency independent and  $\ell^{-1} \propto |\ln T|$ , we conclude that  $\ell$  should be frequency independent at high frequencies with a value  $C_1 = L/|\ln T|$ . In Table I we list the values of  $C_1$  and  $C_2$  obtained by fitting the results of our transfer-matrix calculation of  $\ell^{-1}$  for the four wells plus the mean velocity  $\bar{\nu} = \langle \nu^{-1} \rangle^{-1}$  and the effective-medium velocity  $\nu_0 = \langle \nu_1^{-2} \rangle^{-1/2}$ . The mean velocity is appropriate for the situation where the wavelength is much smaller than the correlation length of the inhomogeneities, whereas  $\nu_0$  would be the infinite wavelength velocity. By Schwarz inequality,  $\nu_0 < \bar{\nu}$ . In the four wells this difference is  $\sim 4\%$ .

One can define a quality factor  $Q = \pi \nu \ell(\nu) / \bar{\nu}$  associated with the attenuation length  $\ell$ . From Eq. (2) and the values of  $C_1$  and  $C_2$  obtained we plot in Figure 3 the frequency dependence of  $Q$ . It is seen that  $Q^{-1}$  has a maximum at 50-150 Hz, and at 20 Hz the localization length is in the range of 10-20 miles, corresponding to an apparent  $Q$  of 300-700. Those values are consistent with previous observations (Schoenberger and Levin, 1978; Menke, 1983). The fact that the loss peak is situated between the seismic and the sonic logging frequencies means that there could be a potential source of velocity dispersion between these two frequency regimes. By assuming that the wave attenuation is accurately described by  $\exp[-\ell^{-1}(\nu)z]$ , we obtain from the Hilbert transform of  $Q^{-1}$  the following frequency dependence of the velocity:

$$\nu(\bar{\nu}) = \bar{\nu} \left( 1 - \frac{\bar{\nu}}{2\pi} \frac{\sqrt{C_2/C_1}}{C_1 \bar{\nu}^2 + C_2} \right), \quad (4)$$

Equation (4) predicts a velocity variation of  $\sim 0.5\%$  between seismic and well-log frequencies. In Figure 4 we show a comparison between the wave-equation solution and the primaries-only synthetic for a 20-Hz pulse in the well Strawberry. The pressure-release boundary condition is applied at the upper interface. Their differences can be attributed to multiple scatterings. It is seen that there is a progressive phase delay of the wave-equation solution corresponding to a  $\sim 2\%$  velocity correction. By examining the time trace from 0-2 seconds for all four wells, we observe that the two seismograms can always be visually re-synchronized if the primaries-only seismogram is stretched appropriately. This stretching is precisely what is accomplished by check-shot corrections in conventional modeling of stacked seismic data. The magnitude of the stretching,  $\sim 2\%$  velocity correction, seems to be larger than the  $0.5\%$  as predicted by Eq.(4) with the fitted values of  $C_1$  and  $C_2$ . However, if we go back to Figure 2 it is seen that there is significant fluctuations in the data, and the observed deviation is within the error range of the data.

#### STATISTICS OF PULSE MULTIPLE SCATTERING

Whereas for a single frequency wave the effect of multiple scattering is to introduce apparent attenuation, the multiple scattering and attenuation of a pulse is associated with additional time-domain characteristics. That is, there is a link between the localization length and the non-stationary power spectrum  $S_r(\nu)$  of the back-reflected signal train, where  $\tau$  is the center of the time window for calculating the power spectrum. In particular,  $S_r(\nu)$  is demonstrated to exhibit the following form:

$$S_r(\nu) = |\hat{f}(\nu)|^2 \cdot \frac{1}{\tau} \mu \left[ \frac{\tau \nu_0}{\ell(\nu)} \right], \quad (5a)$$

where

$$\mu(x) = \begin{cases} \frac{x}{(1+x)^2} & \text{for matched-medium boundary condition} \\ 4x & \text{for pressure-release boundary condition,} \end{cases} \quad (5b)$$

and  $|\hat{f}(\nu)|^2$  denotes the pulse power spectrum. This predicted form of  $S_r(\nu)$  is remarkable in several respects. First, the frequency dependence of  $S_r(\nu)$  is shown to arise directly from the localization length  $\ell(\nu)$ . The knowledge about the form of  $\ell(\nu)$  therefore enables us to predict the spectral frequency variation of the multiple scattering noise. Second, the fact that  $\mu$  is a function of only one variable,  $x = \tau \nu_0 / \ell(\nu)$ , implies that although the multiply back-scattered signal is non-stationary in terms of its statistical variation as a function of time, one can nevertheless scale the spectra obtained at different time windows to a common basis by using the variable  $x$ . One can thus perform averaging over various time windows through the scaling operation. Third, the form of the function  $\mu[\tau \nu_0 / \ell(\nu)]$  given by Eq.(5) tells us that  $\mu$  is really a composition of two functions. The inner function,  $\ell^{-1}(\nu)$ , is particular to the lithology whereas the outer function,  $\mu(x)$ , depends only on the boundary condition. That means even with different wells one can compare and average

the power spectrum data as long as one scales away the material and lithological differences by using the variable  $\chi$ . For a seismic pulse applied at the surface, the backscattered noise spectrum is given by  $\tau^{-1}\mu(\chi)$ , where

$$\mu(\chi) = 4\chi = 4\tau[v_0/l(\nu)]. \quad (6)$$

Since for seismic waves we are in the low frequency regime,

$$l^{-1} = 2\pi^2 v_0^{-2} \alpha \nu^2. \quad (7)$$

Combining Equations (6) and (7) yields

$$N_T(\nu) \propto (\alpha/v_0)\nu^2, \quad (8)$$

i.e. the noise power spectrum  $N_T(\nu) = \mu/\tau$ , when scaled by  $(\alpha/v_0)$ , should display a  $\nu^2$  dependence. In Figure (5) we plot on log-log scales the quantity  $N_T(\nu)/(\alpha/v_0)$  versus the frequency in various time windows, calculated in the pressure-release boundary condition for all the wells. Values of  $N_T(\nu)$  were evaluated from the Fourier transform of the time correlation function for the synthetic seismograms (calculated by using the wave equation), and we have used the Parzen function with a width of ten pulse widths to smooth the correlation function. The solid line has a slope of 2 to guide the eye. It is clear that the scattered points have a definite trend that agrees with the slope 2. To make this point clearer, we take the average of all the points and plot it in dashed line. The agreement with the  $\nu^2$  behavior is indeed surprisingly good.

As a further, more stringent test of the localization theory, we compare the calculated power spectrum  $\mu$  directly with the precise prediction of the theory in the pressure-release case:

$$\mu = 4\chi = 8\pi^2 (\alpha/v_0)\tau\nu^2. \quad (9)$$

In Figure (6) the power spectrum  $\mu$  is plotted as a function of the reduced variable  $\chi$ , where the results of different windows for a given well are averaged to produce a curve. Since in terms of  $\chi$  the function  $\mu$  is universal, all the curves should be compared with the solid line,  $4\chi$ . It is seen that while the scattering is quite significant for each curve, yet when averaged, the dashed curve shows remarkable agreement with the theoretical prediction with no adjustable parameters. The deviation at the low  $\chi$  region could be ascribed to the inaccuracies introduced by the finite time record. Since the theoretical prediction pertains to the expected value of the power spectrum, the behavior of the individual curves and their average is exactly what is expected.

#### CONCLUSION

We have used sonic well-logs to study the effect of multiple scattering and wave localization in stratified lithology. Besides deducing the Q value of multiple scattering attenuation and its frequency dependence, the pulse multiple scattering power spectrum is demonstrated to exhibit the  $\nu^2$  frequency dependence as well as the scaling behavior as predicted by the localization theory. Our results therefore indicate that the localization theory can be

used not only for the estimation of maximum penetration depth of seismic waves, but also for the statistical characterization of the return pulse echoes.

The consequences of this work for modeling seismic data are as follows: the apparent Q's associated with multiple scattering are quite high, from 300-700 (at 20 Hz) for the four wells. These values are consistent with the calculation of others (Schoenberger and Levin, 1978, Menke, 1983). Schoenberger and Levin observed that of 31 wells they analyzed, although three had apparent Q's lower than 200, 28 had apparent Q's equal to or above 200, and most had apparent Q's above 300. Menke performed a simple calculation for a typical sedimentary section, based on his formula for apparent Q, and obtained a value of 640 at 60 Hz.

Our comparisons of primaries-only versus full-wave synthetic seismograms show that the frequency loss in the full-wave seismograms is unobservable from 0.2 seconds. Although the dispersion effect is noticeable, the two seismograms display only a small progressive difference in time, which can be tracked well enough that the two seismograms can always be visually re-synchronized by an appropriate local time shift. In some places, the two seismograms differ even after supplying a time shift, due to the local interference of longer period multiples, but these effects are small.

All of these results confirm that for modelling stacked seismic data, in which the effects of longer-period multiples are suppressed, the check-shot correction should introduce the appropriate time delays to synchronize the primaries-only synthetic seismogram with the field data.

#### ACKNOWLEDGMENT

We would like to acknowledge Warren Ross and Pravin Shah, Exxon Production Research Co. for providing well log data, and for useful discussions. Two authors (P. Sheng and B. White) wish to thank Frank Levin for his encouragement/helpful conversations.

#### REFERENCES

- Anderson, P. W., 1958, Absence of diffusion in certain random lattices: *Phys. Rev.* 109, 1492-1505.
- Burridge, R., Papanicolaou, G., and White, B., 1987, Statistics for pulse reflection from a randomly layered medium: *SIAM J. Appl. Math.* 47, 146-168.
- Burridge, R., Papanicolaou, G., Sheng, P., and White, B., 1987, Probing a random medium with a pulse: submitted to *SIAM J. Appl. Math.*
- Godfrey, R., Muir, F., and Rocca, F., 1980, Modeling seismic impedance with Markov chains: *Geophysics* 45, 1351-1372.
- Goldman, A. M., and Wolf, S. A., Eds., 1984, Percolation, localization, and superconductivity: NATO ASI Series vol. B109, Plenum Press.
- O'Doherty, R. F., and Anstey, N. A., 1971, Reflections on amplitudes: *Geophysical Prospecting* 19, 430-458.

Menke, W., 1983, A Formula for the Apparent Attenuation of Acoustic Waves in Randomly Layered Media: *Geophys. J. Res. Astr. Soc.* 75, 541-544.

Richards, P. G., and Menke, W., 1983, The apparent attenuation of a scattering medium: *Bull. of the Seismological Soc. of Am.* 73, 1005-1021.

Schoenberger, M., and Levin, F. K., 1974, Apparent attenuation due to intrabed multiples: *Geophysics* 39, 278-291.

Schoenberger, M., and Levin, F. K., 1978, Apparent attenuation due to intrabed multiples, II: *Geophysics* 43, 730-737.

Sheng, P., White, B., Zhang, Z. Q., and Papanicolaou, G., 1986, Minimum wave-localization length in a one-dimensional random medium: *Phys. Rev. B* 34, 4757-4761.

Sheng, P., Zhang, Z. Q., White, B., and Papanicolaou, G., 1986, Multiple scattering noise in one dimension: universality through localization length scaling: *Phys. Rev. Lett.* 57, 1000-1003.

White, B., Sheng, P., Zhang, Z. Q., and Papanicolaou, G., 1987, Wave localization characteristics in the time domain: *Phys. Rev. Lett.* 59, 1918-1921.

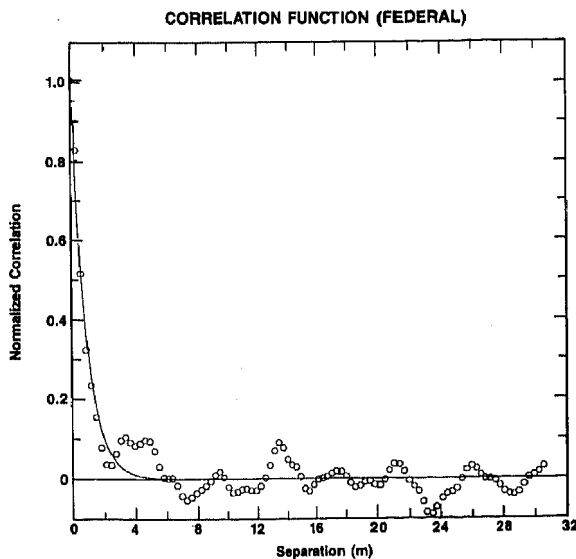


FIG. 1. Autocorrelation function plotted as a function of separation for federal at depth of 2247 m. Solid line is exponential fit.

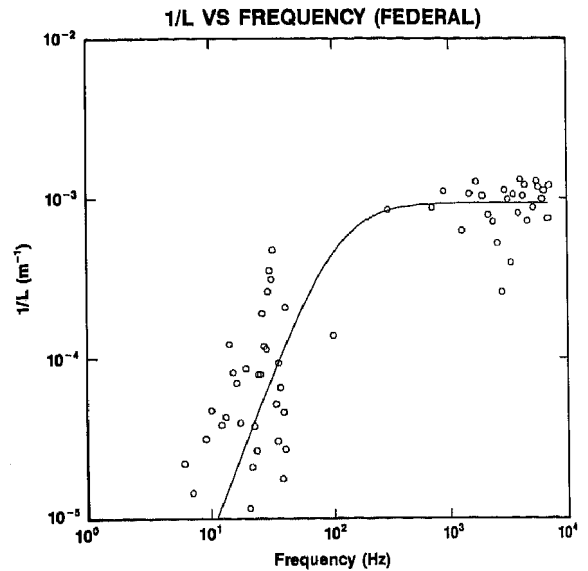


FIG. 2. Data for  $\ell^{-1}$  vs. frequency. Solid line is fit.

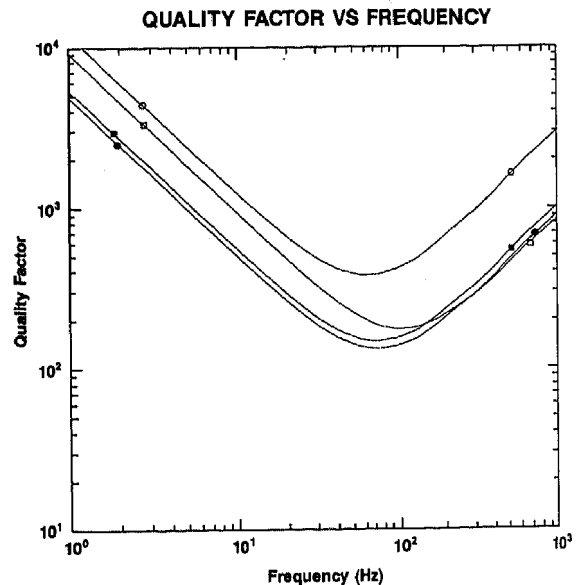


FIG. 3. Quality factor for multiple-scattering attenuation plotted as a function of frequency.

□ = Federal  
○ = Inigok  
● = Hornbeck  
■ = Strawberry

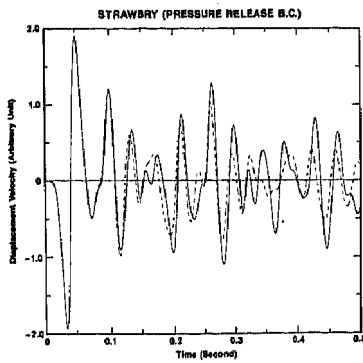


FIG. 4. Comparison of full wave-equation solution (solid line) and the primaries-only reflection series (dashed line).

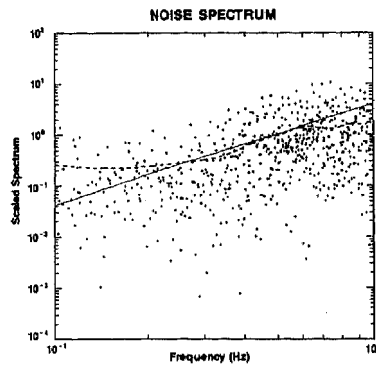


FIG. 5. Scatter plot of  $N(r)/(\alpha/v)$ . Solid line has a slope of 2 to guide the eye.

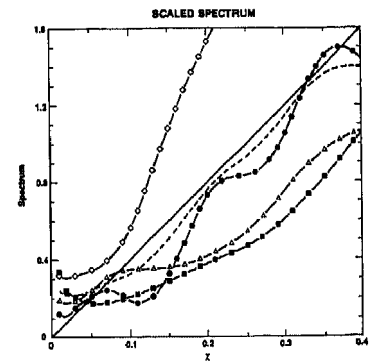


FIG. 6. Multiple scattering power spectrum plotted in reduced variable.

$\Delta$  = Federal  
 $\blacksquare$  = Strawbry  
 $\bullet$  = Hornbeck  
 $\diamond$  = Inigok  
 Solid line is theory, dashed line is average of 4 curves.

Table 1. Localization constants and  $v$  and  $v_0$  for the 4 wells.

Constants	$C_1$ (m)	$C_2$ (m - Hz <sup>2</sup> )	Mean Speed $v$ (m/sec)	Effective-Medium Speed $v_0$ (m/sec)
Wells				
Federal	1080	$1.18 \times 10^7$	4102	3941
Strawbry	1759	$9.36 \times 10^6$	5557	5367
Hornbeck	1074	$5.82 \times 10^6$	3832	3654
Inigok	3447	$1.37 \times 10^7$	3651	3479